ADVANCED MATERIALS
www.advmat.de

Electrical Textile Valves for Paper Microfluidics

*Alar Ainla, Mahiar M. Hamedi, Firat Güder, and George M. Whitesides**

This paper describes electrically-activated fluidic valves that operate based on electrowetting through textiles. The valves are fabricated from electrically conductive, insulated, hydrophobic textiles, but the concept can be extended to other porous materials. When the valve is closed, the liquid cannot pass through the hydrophobic textile. Upon application of a potential (in the range of 100–1000 V) between the textile and the liquid, the valve opens and the liquid penetrates the textile. These valves actuate in less than 1 s, require low energy (≈27 µJ per actuation), and work with a variety of aqueous solutions, including those with low surface tension and those containing bioanalytes. They are bistable in function, and are, in a sense, the electrofluidic analog of thyristors. They can be integrated into paper microfluidic devices to make circuits that are capable of controlling liquid, including autonomous fluidic timers and fluidic logic.

Paper microfluidics is a technology that is particularly well-suited for use in public health, diagnostics for resource-limited settings, veterinary medicine, testing of food and water quality, and environmental monitoring.[1–8] Many common assays require the addition of multiple reagents and multiple washing steps, where the timing of each step influences the outcome of the assay. For example, paper-based devices for enzyme-linked immunosorbent assay (ELISA),[9–13] electrochemiluminescence (ECL),[14] or DNA detection,[15,16] require multiple individually timed steps of binding, washing, and amplification. Performing these steps manually is labor intensive (a single assay may take from several minutes to hours) and prone to human errors. Fully automated paper-based assays have the potential to be faster and more accurate than those requiring human operations.

The most important component required for autonomous assays is a fluidic valve that gates the flow of liquids with timed actuation. Different methods of valving have been explored for paper devices,[17–24] which operate either by changing the wicking properties of the paper or by mechanically altering connectivity between the channels. Wicking speed in the paper is determined by three parameters: the hydrophilicity of its surface, the size of the pores, and the viscosity of the liquid. These parameters can be altered to actuate flow of liquids. For example, hydrophobic surfaces can be rendered hydrophilic by an electrical plasma[17] or by electrochemical[18,25] or ultraviolet modification.[26] Surfactants can also be used to assist liquids in crossing the hydrophobic barriers;[24,27,28] dissolved polymers[29] or sugars[30] can increase the viscosity of the liquids and limit the flow.

Mechanical motion of paper has also been used for actuating the flow of liquids in paper. Electromagnetic,[19] hygroexpanding,[20,31] manually operated push-buttons,[21] flaps,[22] pop-up,[32] folding,[10,33] and sliding-strip[15] concepts for valving have been reported in the literature (for a more complete list of published work see Table S1, Supporting Information). Valves that involve soluble substances, such as surfactants, or chemical modifications, like plasma, or electrochemistry, are more prone to influence the reagents used in the assays compare to purely physical methods, such as mechanical motion. Mechanical valves, such as manually operated push-buttons or cantilevers do not have this drawback, but mechanical parts are more prone to failure than chemical ones, and they cannot be controlled using simple electronics.

This paper describes an electrically actuated valve based on a fine electroactive mesh or a textile fabricated from woven fibers, whose wettability can be controlled by application of a voltage (**Figure 1**). We call this mesh an "electrotextile" and describe its fabrication and properties below.

Electrotextile-based valves have four characteristics that have the potential to be useful in paper devices: i) they are controlled electronically (e.g., they require no mechanical parts); ii) they are simple and inexpensive to fabricate; iii) they can be integrated with paper microfluidics; and iv) they operate rapidly (i.e. they actuate in <1 s).

We show that this new class of valves can be integrated into paper microfluidic devices, and use the valves as a building block for fabricating devices of higher complexity such as circuits that contain valves in series and parallel configurations. We also demonstrated circuits with timed-actuation and a self-regulation (i.e., logic NAND gate) for fluidic logic. We also constructed a battery-operated, portable control unit for the actuation of the valves using off-the-shelf electronics.

To characterize the electrowetting in the electrotextile valves, we used woven textiles that contain metallic fibers or plastic fibers having a conductive metal coating. We also explored conductive paper (Table S2, Supporting Information) but concluded that electrotextiles were easier to prepare and more consistent in their performance. All the materials were coated with Parylene-C[34,35] for electrical insulation between the liquid and the metal, and Teflon AF,[36] to increase the hydrophobicity of their surfaces (see **Table 1**).

We measured the break-through pressure of water for different electrotextiles using a simple device in which we

Dr. A. Ainla, Dr. M. M. Hamedi, Dr. F. Güder, Prof. G. M. Whitesides
Department of Chemistry and Chemical Biology
Harvard University
Cambridge, MA 02138, USA
E-mail: gwhitesides@gmwgroup.harvard.edu

The ORCID identification number(s) for the author(s) of this article can be found under https://doi.org/10.1002/adma.201702894.

DOI: 10.1002/adma.201702894

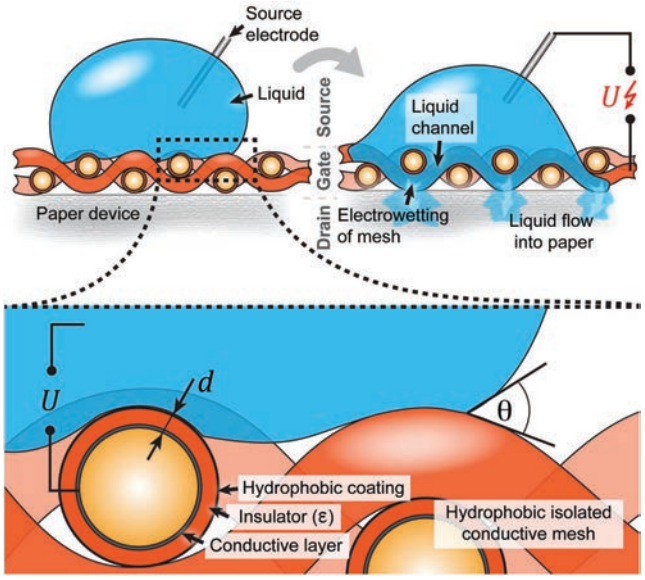

Figure 1. Principle of the bistable electrical valve. Schematic diagram of the operation of the valve, which is based on the principles of electrowetting on dielectric (EWOD). The gate electrode is a conductive textile covered with layers of insulator and hydrophobic coating ("electrotextile"). This electrotextile is not permeable to liquid. The application of a voltage between the liquid and the electrotextile allows liquid to flow into the paper layer underneath due to electrowetting.

increased the applied pressure by increasing the height of a column of water, placed on top of the textile until the valve opened (without using electrical actuation; see Figure S1, Supporting Information). We found that the break-through liquid pressure was in the range of 6–12 mbar (0.6–1.2 kPa) for the materials that we tested (see Table 1 and S2, Supporting Information). We then investigated the threshold of voltage for actuation, for the different materials, using deionized water (see experimental details, and Figure S3, Supporting Information); we determined that a potential between 100 and 1000 V activated all of the different electrotextiles. The break-through pressure of the hydrophobic textiles was sufficiently high to allow containment of liquids for applications in microfluidics.

This valve is bistable. Once a flow is initiated due to electrowetting, it cannot be stopped until the entire volume of liquid flows across. We confirmed the bistable character of the valve by running several (up to five) actuation cycles in series. For each cycle, we deposited a drop of liquid onto the electrotextile valve. The liquids did not pass the valve until an actuation pulse of 300 V for 0.5 s was applied (Figures S7 and S8, Supporting Information). The flow of liquid continued until the entire drop passed through the valve (i.e., well after the pulse had ended). After 30–45 s (after the flow had ceased), the valve dried up, and the cycle could be repeated.

To understand the behavior of electrowetting through electrotextiles better, we developed a theoretical model for the operation of this new class of valves, inspired by the principles of electrowetting-on-dielectric (EWOD).[37–49] EWODs have been widely studied and used in the field of "digital microfluidics" for handling of liquids on planar surfaces. In our case, however, the valves do not have planar surfaces and instead operate based on the principle of penetration of liquids through porous materials with the help of electrowetting. This type of materials has not, to our knowledge, been used previously for microfluidics. To describe this complex process with a simple model, we combined the Washburn equation[50] with the Lippmann–Young equation for EWODs,[47] and derived an analytical expression (Equation (1); see the Supporting Information for details) for the activation voltage U_a required to trigger flow of liquid through the electrotextile

$$U_a = \sqrt{-\frac{2\sigma d_i \cos\theta_0}{\varepsilon\varepsilon_0}} \quad (1)$$

θ_0 is the stationary contact angle of water on the planar surface of the electrotextile material (Teflon-AF), ε is the dielectric permeability of the layer of insulation on the wires (3.15 for Parylene-C), d_i is the thickness of the insulation layer (≈10 µm Parylene-C), and σ is the surface tension of the liquid.

To test this theory, we used mixtures of ethanol (EtOH) and water to vary the surface tension of the liquid σ_i = 72 mN m^{-1} (water), 56 mN m^{-1} (5% EtOH), 48 mN m^{-1} (10% EtOH), 28 mN m^{-1} (50% EtOH), and measured the actuation voltage for each liquid using an aluminum electrotextile coated with Parylene-C (11 µm) and Teflon AF (see **Table 2**). As expected,

Table 1. Properties of the three woven materials for electrowetting.

Property	Copper textile	Aluminum textile	Polyester textile metal plated
Electrical conductivity	Intrinsic	Intrinsic	Zn/Ni/Cu plating
Insulation layer		≈10 µm Parylene-C	
Hydrophobic layer		Dip coated with Teflon AF 2400	
Resistivity [Ohm per square]	≈10^{-8}	≈10^{-8}	0.1
Fiber diameter [µm]	136	71	22
Mesh opening size [µm]	143	62	157
Mesh period [µm]	279	136	179
Thickness [µm]	300	180	60
Liquid breakthrough pressure (mbar)	10.1 (σ = 3.4)	18.8 (σ = 4.1)	6.1 (σ = 2.0)
Cost [USD cm^{-2}]	0.018	0.03	0.0042

Table 2. Measured actuation voltage for an aluminum textile (according to Table 1) for different solutions.

Solution	Surface tension [mN m^{-1}]	Actuation voltage (standard deviation, $n = 7$)
Water	72	450 (320)
5% EtOH in water	56	300 (210)
10% EtOH in water	48	141 (75)
50% EtOH in water	29	80 (21)
EtOH	22	–
1×10^{-3} M pluronic F68 in PBS		188 (45)
BSA (50 g L^{-1}) in PBS		480 (330)
Blood		240 (63)

the actuation voltage decreased with lower surface tension (according to Equation (1)). Interestingly, the standard deviation of the actuation voltage also decreased monotonously with decreasing surface tension. Equation (1) can estimate the voltage for actuation for different materials and liquids, and describe the trends, but it does not provide exact numbers (see Figure S4 in the Supporting Information). To describe electrowetting through textiles, we believe that an improved theory would be useful—one in which the Lippmann–Young equation is replaced with a model that fits the 3D microscale geometries used here. A more accurate model than the Washburn equation would describe the pressure required for a liquid to penetrate the textile.

We also used the aluminum electrotextile (Table 2) to determine the valving behavior for solutions with different compositions (which may be relevant in various bioanalytical assays). We tested solutions of Pluronic F-68, which is an example of a surfactant used in some bioassays. The use of surfactant reduced the actuation voltage and the standard deviation. We tested solutions of bovine serum albumin (BSA), as an example of a protein-containing solution. The BSA solutions penetrated through the valve upon actuation with actuation voltages similar to that of water, and demonstrated that the higher viscosity does not affect electrowetting. We also tested human whole blood, which also actuated, showing that complex bodily fluids, containing cells, can pass through the pores of the woven textile.

After having established that bistable valves can be fabricated using electrotextiles, we integrated the valves and other relevant components into paper microfluidic devices. This integration was achieved by stacking paper with microfluidic structures, with electrodes printed on its surface, together with electrotextiles, into multilayer devices (see experimental details and **Figure 2**A).

The most basic components that can be implemented with this fabrication technique are printed electrodes/wires[51] and paper-based microfluidic channels.[52] By adding two more basic components—the electrical valve and a fluid-to-electrical switch (this component switches an electrical signal using a liquid input)—we could design and fabricate simple integrated circuits. In these circuits liquids and electrical signals could control each other interchangeably, so we term them "printed electrofluidic circuits." Because of the bistable nature of the valves, they are functionally analogous to semiconductor thyristors, which are devices used widely in AC power electronics (and not analogous to the transistors used much more widely in binary information processing). A thyristor switches "on" quickly when a voltage

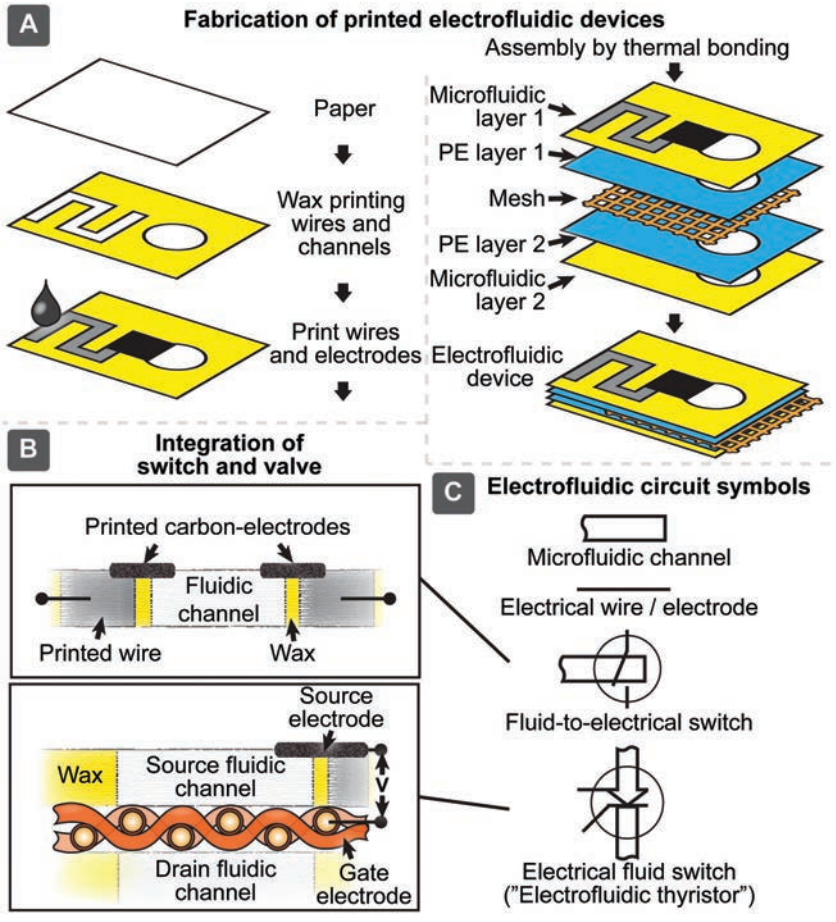

Figure 2. Design and fabrication of printed electrofluidic devices. A) Schematic diagram of the fabrication of 3D printed electrofluidic circuits. Microfluidic channels are printed using wax printing, followed by printing of electrodes (for valves and switches) and electrical wires on the paper layers. Conductive, insulated, and hydrophobic "electrotextiles" are then bonded with the paper layers using hot-lamination with polyethylene films. B) Schematic cross-section of a fluid-to-electrical switch, and schematic cross-section of an integrated valve containing two microfluidic layers and a valve layer. The valve is actuated when a voltage is applied between the liquid ("source electrode") and the electrotextile ("gate electrode") whereupon liquid can pass from the "liquid source" into the "liquid drain." C) Circuit diagram symbols for printed microfluidic channels, printed wires/electrodes, integrated fluid-electrical switches, and valves ("electrofluidic thyristors").

pulse is applied to its gate electrode and remains open as long as a positive electrical potential is present between the cathode and anode. Inspired by the electronic symbol for the thyristor, we have designed a symbol for the textile valve where the gate is an electrical conductor made of a solid material, and the anode and cathode are represented as fluidic channels. We call this an "electrofluidic thyristor" (Figure S7, Supporting Information). Figure 2C shows the proposed circuit diagram symbol for all the electrofluidic components.

We integrated the electrofluidic switch and valves using these design principles (see Figure 2B): i) A fluid-to-electrical switch: We fabricated this switch by printing two carbon electrodes separated by a microfluidic channel in between. When there is no electrically conducting liquid (e.g., aqueous solution) present in the channel, the dry paper does not allow flow of significant electrical current from one electrode to the other, essentially rendering the switch "off." Low currents are still possible due to the spontaneous conductivity of paper,[53] but in our observation, this conductivity is not sufficient for valve operation. The flow of larger electrical current is only possible when a liquid electrolyte is present in the channel, turning the switch "on." ii) An electrofluidic valve: The basic design for the valve consisted of a three-layer structure, where the electrotextile was sandwiched between two sheets of paper with wax-printed microfluidic structures (Figure 2). We printed carbon electrodes in the liquid reservoirs in the top layer, which acted as individual electrodes ("source") for each valve. The electrotextile in the middle layer was connected to ground ("gate"). Liquids placed in the reservoir do not penetrate through the middle layer until a voltage pulse is applied to activate the valve and allow the liquid to flow through to the bottom microfluidic layer.

The behavior of fluids in these valves is dominated by capillarity for the relatively small amounts of liquid volume that we use, and gravity should not have a large effect on the valving. To determine the effect of gravity we tested several paper devices at different angles vs. gravity (see methods). As expected the valves operated at all angles from 0° to 180° (upside down) and the voltage for activation was independent of the angle (Figure S9, Supporting Information).

The electrofluidic thyristor provides a building block that can be integrated into 3D circuits in various configurations for applications involving paper-based microfluidics. Integrating these valves, in series or in parallel, allows fabrication of devices with a greater complexity.

Figure 3 demonstrates the integration of the valves in parallel. Here two valves were fabricated on the same layer. Each valve has an individual reservoir for liquid, and we could operate them individually and deliver each liquid to a common microfluidic channel. This configuration could allow the time-controlled addition of multiple solutions and reagents to an assay, as seen in Figure 3D.

Figure 4B,C shows serially connected valves fabricated using a five-layer configuration. This device uses two separate electrotextiles for each valve (in layer 2, and layer 4). It is essentially a vertical flow device, in which the first valve passes the fluid from layer 1 to layer 3, and the second valve passes the fluid from layer 3 to layer 5 (see Figure 4 D). Such architectures could be used for assays involving multistep reactions.

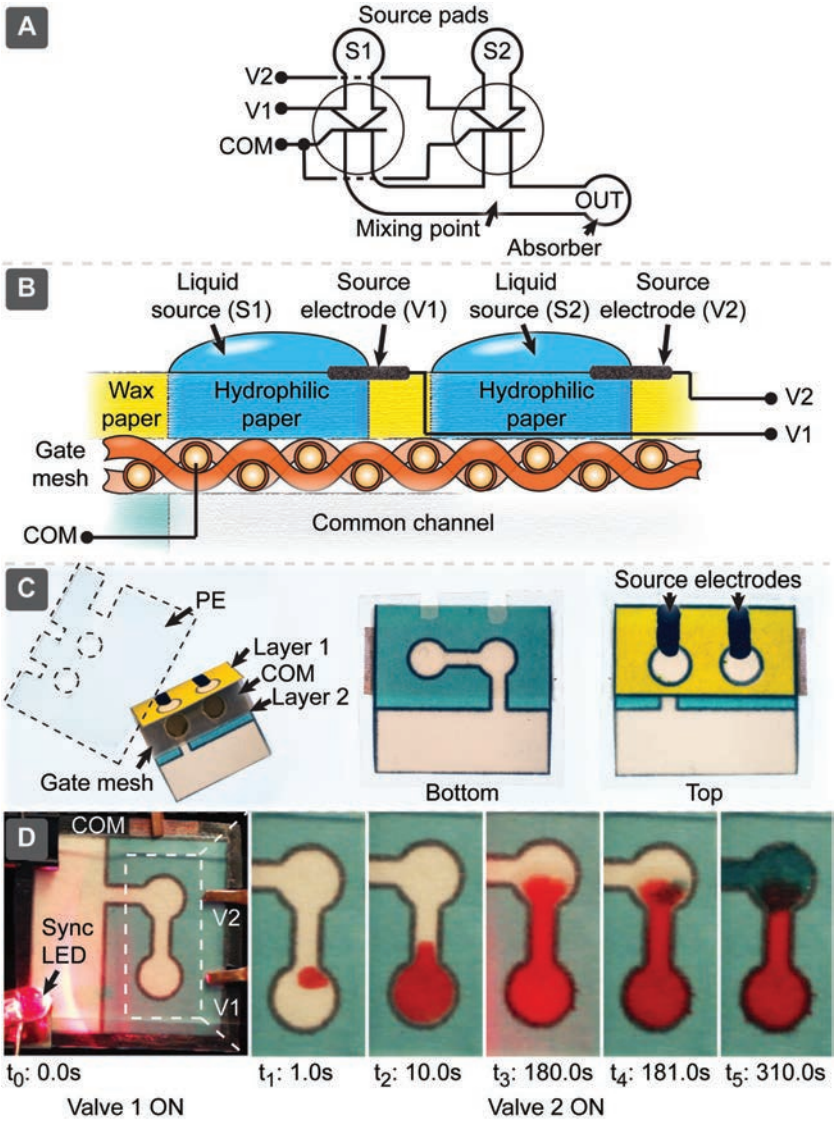

Figure 3. Valves in parallel connection. A) Circuit diagram of two individually addressable electrofluidic valves connected to a common drain channel. B) Schematic cross-section of the device. C) Photos of the fabrication process. The devices were printed on a single sheet of paper, which was folded around the electrotextile and laminated using polyethylene films. D) Photographs of the operation of the device where two aqueous solutions in separate reservoirs (red and green) are injected into a common channel. A LED indicates when an electrical pulse is applied to open each valve.

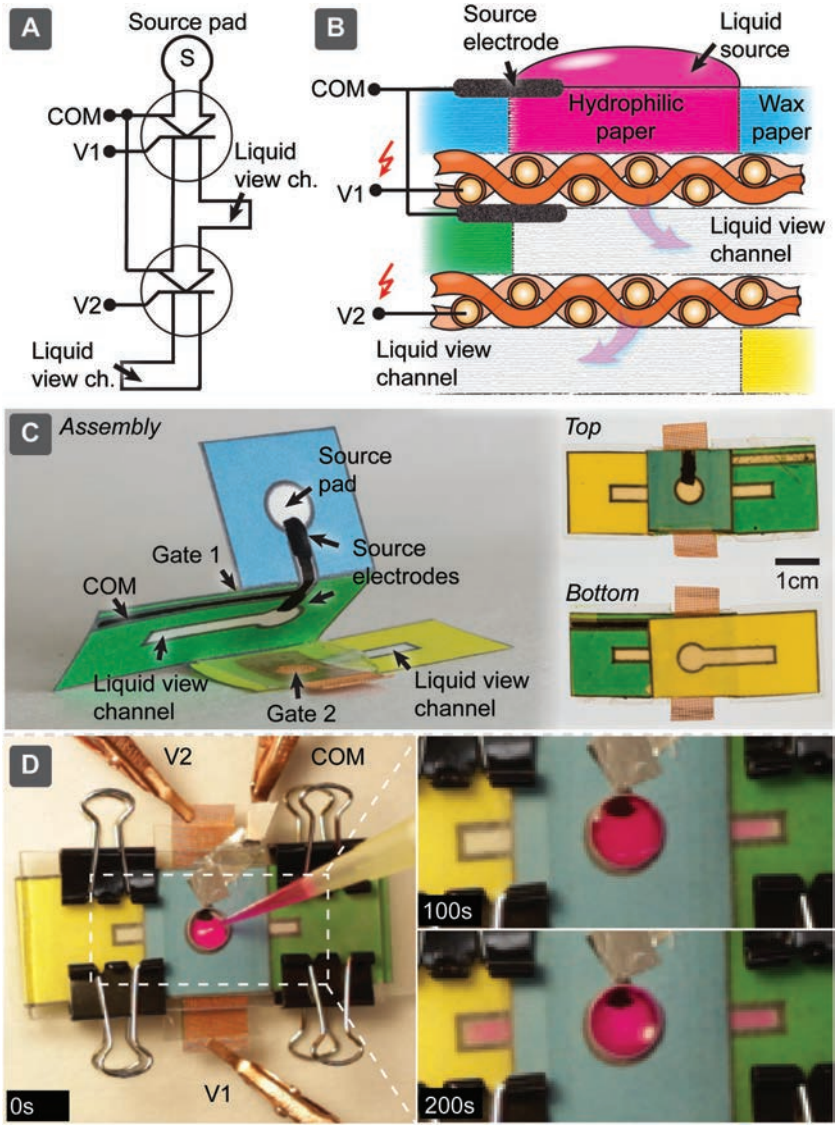

Figure 4. Valves in serial connection. A) Circuit diagram of two individually addressable electrofluidic valves connected in series. We have used liquid view channels to visualize the presence of liquid in the middle layer, which would otherwise not be visible due to the stacked structure. B) Schematic cross-section of the device containing three microfluidic layers separated by two layers. C) Photographs of the device fabrication where we printed the microfluidic channels on a single sheet of paper, folded the paper around the electrotextile and laminated the device with polyethylene films. D) Time-lapse photographs showing the operation of the device, where the liquid passes the first valve (by applying a voltage V1), and thereafter the second valve (by applying a voltage V2).

We show two examples of self-regulating electrofluidic paper chips. The advantage of such devices was that no external circuitry is required for controlling the timed signals. Instead the timing and logic functions and signals are generated in the paper device itself.

In the first example, we fabricated a fluidic timer ("fTimer"), shown in **Figure 5**A,B. We demonstrate this device because autonomous timing of liquids is important for many applications, and a number of approaches have already been demonstrated.[24,28] The fTimer device is activated when water is added to a microfluidic channel, which acts as the timer. The liquid wicks along the channels at a speed determined by the properties of the paper and the fluid, and turns on a number of fluid-to-electrical switches along its path. Each switch triggers a valve and allows flow of three different liquids into a common output channel (Figure 5C,D,E).

The second example demonstrates a logic flow control, which would allow actuating the valve depending on simple binary input conditions, presence (logic state "1") or lack (logic state "0") of the liquid in the inputs. Our logic flow-control circuit performs Boolean NAND operation (we can also call it fluidic NAND gate, or simply fNAND). The NAND gate is the fundamental building block of all digital logic and any digital circuit element can be constructed using a combination of NAND gates alone. The difference between the fNAND and an electronic NAND is that the inputs and outputs of the fNAND are encoded by the presence of the fluid in channels, instead of electrical voltage between wires. The main limitation of paper-based logic flow-control is that the state of each gate can be evaluated only once. Wicking is a one-way process and filling of paper channels is irreversible, which means that any given state can only transition from "0" to "1," but not vice versa. This requires that evaluation of the logic gate is triggered and output is only generated after a clocking signal (**Figure 6**A; Figure S10A, Supporting Information). Corresponding equivalent in electronics would be NAND gate with output couple through a D flip-flop (Figure S10B, Supporting Information). D flip-flops copy their input (D) to output (Q) only during the rising-front (transition from "0" to "1") of clocking signal (CLK), while output remains unaffected during both the low and the high CLK states. Similarly, our fNAND gate has one output valve, which is triggered by the clock. The valve is not actuated only when both inputs (A and B) are in state "1" during the rising clock signal, since NOT ("1" AND "1") is "0."

Paper microfluidics are most practical in settings where portability, simplicity of operation, and affordability are crucial. We and others have proposed simple portable electronic devices that are capable of performing advanced electroanalytical tests on paper microfluidic devices.[54] The ability to control the valve with a simple, portable device is therefore important. Even though the valves require relatively high actuation voltage (up to 600 V), we have constructed a simple electronic power supply, with a cost of materials less than 10 USD, that can be operated from a single 1.5 V AA battery (Figure S11, Supporting Information) and deliver the appropriate voltage. All the essential components of the power supply

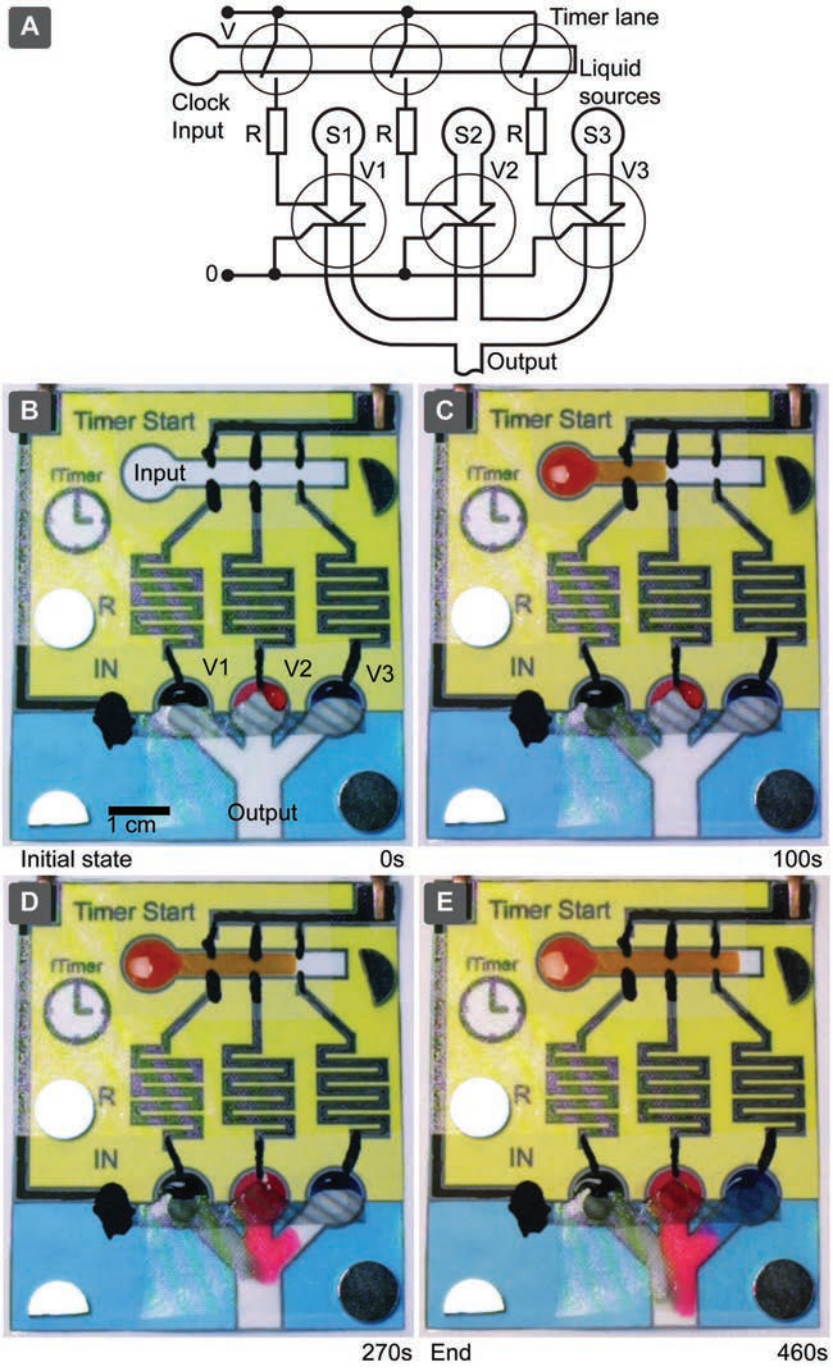

Figure 5. Electrofluidic timer. A) Circuit diagram of a fluidic timer. B) Photograph of a fluidic timer device. C–E) Time-lapse photographs of the device where the liquid propagation (orange liquid) in the timer channel trigger sequential addition of three colored liquids (black, red, blue) from three reservoirs into a common output, by opening a valve for each liquid (V1, V2, V3).

were extracted from a disposable photo camera (Figure S11, Supporting Information).

We calculated that the energy required for actuation of the valves is around 27 μJ (the experimental requirements of energy were measured to be slightly higher due to leakage currents, but nonetheless less than 1 mJ per actuation—see Supporting Information). The low power consumption is one of the advantages of the valves. A single battery could power many paper chips with our portable device (Estimated about 20 000 cycles, see Figure S11, Supporting Information for details).

Finally, we demonstrated the valve in an iodate assay reported by Lieberman and co-workers.[55] Briefly, this assay is composed of the analyte (KIO_3^-), three reagents (p-toluenosulfonic acid, KI, $Na_2S_2O_3$), and a starch indicator that produces the colorimetric output signal. In this assay, the excess iodide reacts with the iodate in the acidic environment and forms triiodide (Equation (2)). Triiodide is then titrated with thiosulfate (Equation (3)); if the amount of triiodide exceeds the reducing capacity of the thiosulfate, the indicator starch turns blue (Equation (4)), and if the amount of triiodide is smaller the indicator remains uncolored

$$IO_3^- + 6H^+ + 8I^- \rightarrow 3I_3^- + 3H_2O \quad (2)$$

$$I_3^- + 2S_2O_3^{2-} \rightarrow 3I^- + S_4O_6^{2-} \quad (3)$$

$$I_3^- + \text{starch} \rightarrow \text{blue complex} \quad (4)$$

In this assay, the analyte and reagents should be mixed first and the product should be applied to the indicator area for evaluation in a timed manner. To integrate this assay in a paper device, we dried the reagents in different zones in an input pad (since the reagents are mutually incompatible). For mixing we place 40 μL of analyte on the input pad. This amount of liquid was sufficient to cover the entire input pad and connect the individual zones. Since paper could not absorb the entire volume in its pores, an open drop left outside of the paper matrix would support convective mixing upon mechanical agitation. For timing, we integrated a valve that was actuated 3 min after mixing to bring the product into an indicator pad, where a colorimetric output signal was generated (see **Figure 7**, and experimental section). The timing was controlled digitally in the voltage generator device, since we think it is feasible that paper devices would be interfaced with digital electronics (e.g., cell phones). It should however be easy to integrate a fluidic timer (similar to the device that we demonstrated in Figure 5) with the iodate assay for a more autonomous device that would only rely on a voltage source without any additional electronic circuitry. We designed the reagent concentrations for a test that would be

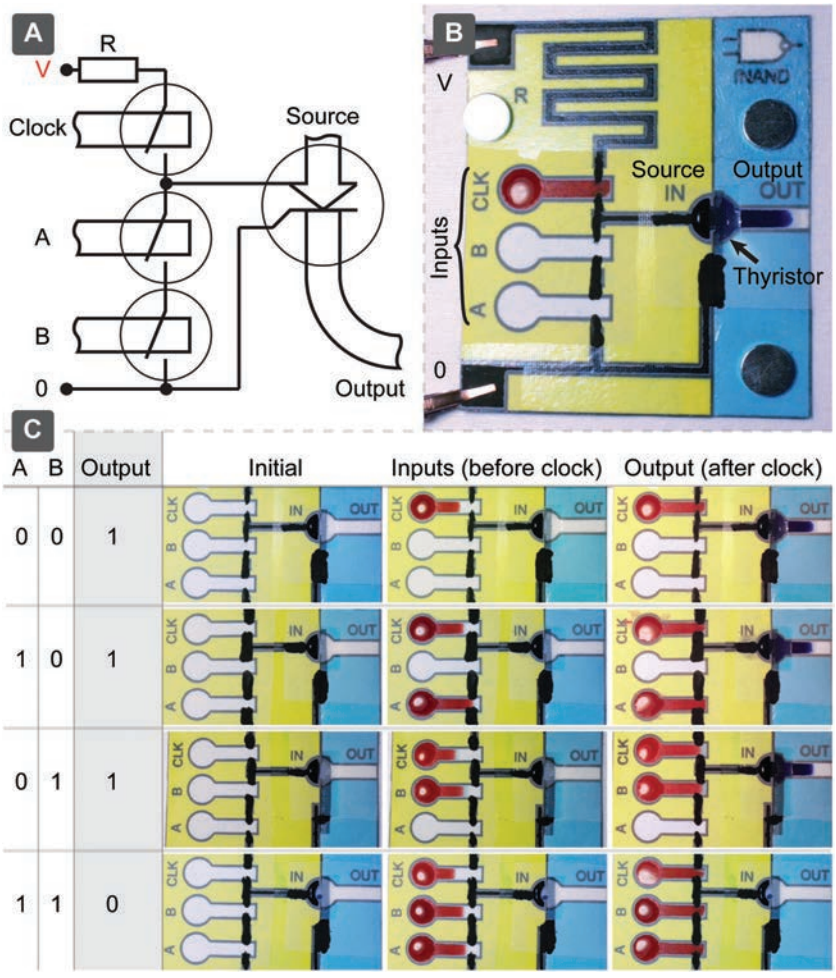

Figure 6. Electrofluidic NAND gate (fNAND). A) Circuit diagram of a fluidic NAND, and B) Photograph of a synchronous fluidic NAND gate. The logical state (1) is represented by the present of a liquid in the inputs (A and B) or output (OUT), and the lack of liquids represents the logical state (0). The device is triggered by addition of a liquid to the clock input (CLK). C) Photographs of all four logical states of the device. The input liquids are red, and the output liquid is blue.

useful for analyte concentration of around 1×10^{-3} M (see Supporting Information). Figure 7C shows the results for 0×10^{-3}, 1×10^{-3}, and 5×10^{-3} M analyte concentrations tested using the integrated devices. Note that even the test with pure water shows a background color although no color signal is produced in paper. The reason is that a wet paper layer is more translucent making the darker gate mesh visible in the signal. Tests with indicator pads, which do not have the gate mesh do not show this background. This problem could be addressed by designing a white gate mesh. The iodate assay shows the possibility of integrating valves into paper-based assays, and we envision that other assays, which may even require several timing steps, and thus several valves, can be realized (see e.g., Figure S17, Supporting Information for a possible scheme to use in integrating an ELISA-based assay using two valves in parallel connection).

This paper demonstrates electrical valves based on hydrophobic electrotextiles (an electrically conductive textile, presenting an electrically insulating and hydrophobic surface coatings) that can be integrated into 3D-paper-based microfluidic devices. When the valve is "off," a liquid (aqueous solutions) cannot pass through the electrotextile. When an electrical potential is applied between the electrotextile and the liquid, the liquid can penetrate through the textile due to electrowetting. This phenomenon is different from previously demonstrated electrowetting on dielectrics, which works on planar surfaces.[46] These valves have five advantages: i) They can easily be integrated into multilayer printed microfluidic devices; ii) They are sufficiently fast for applications in microfluidics (they actuate in less than 1 s), and they require little power (100 μW or less) for operation; iii) They have no moving parts; iv) They do not react chemically with the aqueous solutions upon actuation; v) They work with different aqueous solutions including low-surface-tension liquids (water with 50% ethanol), solutions containing surfactants, and bioanalytes. Their main disadvantages are that they require high voltages (100–1000 V), are bistable, we cannot control the flow rate, they are effectively irreversible, and they cannot be closed before the liquid in the channel completely passes through the valve.

We have also demonstrated paper microfluidic circuits with several valves integrated to form: i) autonomous fluidic timers, and ii) logic fluid flow-control led devices without the need for an external electronic control logics or processor. We have also shown a small, low-cost, and portable electronic device that can deliver high voltages for controlling the valve and that operates with a single AA battery.

Integration of electrotextile valves in paper-based microfluidics will be especially interesting to explore in applications where timed multistep reactions are required, such as in paper-based ELISA,[9,10] ECL,[14] or nucleic acid biosensors.[15] We believe that electrotextile valves are also suitable for other microfluidic and lab-on-a-chip systems that are based on thin materials,[56,57] or open-channel paper microfluidics.[58–60] Electrotextiles would be best suited for fabrication by lamination, and thus compatible with processes that fabricate paper and foil devices. Bonding the textile layer between the silicone slabs (such as PDMS) is more cumbersome than lamination with thermoplastics and hot pressing. For silicone devices, the best-established approach is channel closure by pinching either by pneumatics[61] or mechanical pins.[62] Elastomeric valves are advantageous as they can be quickly opened and closed reversibly, but suffer from more expensive and complicated electromechanical control units than the simple high-voltage power source required for valves presented here.

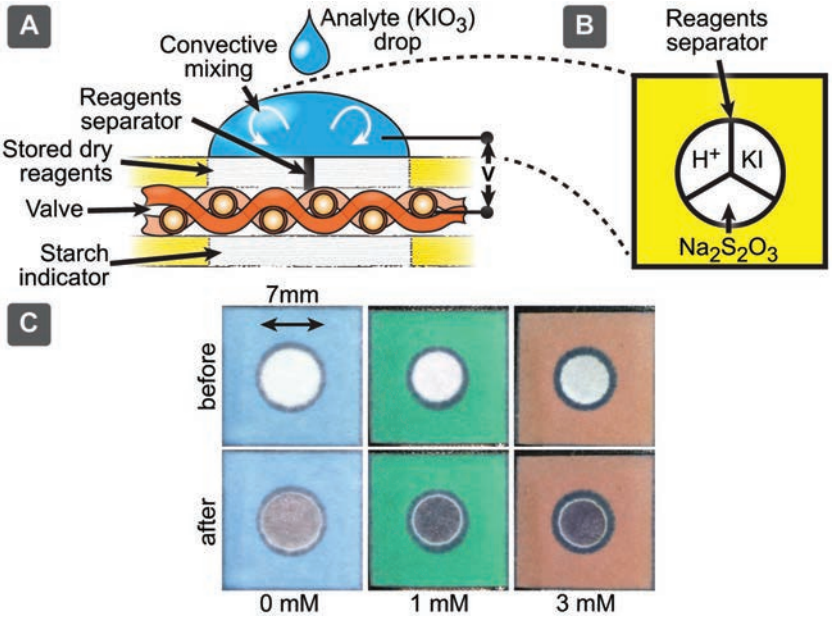

Figure 7. A) Schematic diagram of the integrated iodate assay device. To operate the device, we first add the analyte (KIO_3) to the input pad (B) composed of three separated areas, that each store the individual components H^+, KI, and $Na_2S_2O_3$. The analyte volume is sufficiently large to allow convective mixing of the components upon mechanical shaking. After mixing (3 min), we open the valve and the product is transferred to the starch indicator pad. C) Photographs of the device showing colorimetric signal depending on the analyte concentration.

Experimental Section

Materials: Woven copper (product code: 9224T819) and aluminum (product code: 9224T819) woven textiles were purchased from McMaster-Carr. Plastic textile with a conductive coating (VeilShield) was purchased from LessEMF Inc. This material was based on polyester threads, which were woven with large spacing and bound together through melting to avoid sliding or separation of threads. This material had conductive electroplated metal (Zn/Ni/Cu) coating. Lens Paper (Whatman 105) was purchased from Sigma-Aldrich (we measured all geometrical parameters of materials using macro photography and a digital caliper). 2% starch indicator was obtained from VWR. 1 M p-toluenosulfonic acid, 0.5 M KI, and 30×10^{-3} M $Na_2S_2O_3$ were prepared in milli-Q water.

Preparations of Different Materials for Valves: For electrical insulation, all valve materials were coated with Parylene-C (Paratronix Inc., Attleboro, MA). A hydrophobic coating was applied to surfaces using soluble fluoroplastic DuPont Teflon AF (Details of coating procedures are given in supplementary information). Teflon was chosen AF because it has a low surface energy (the contact angle of water on Teflon AF $\theta_{H_2O} = 105^{\circ}$).

High Voltage Power Supply: A Keithly 2410 Source-meter or self-built custom low-cost power-supply (Figure S11, Supporting Information) was used as a single channel voltage source up to voltages 1.1 and 0.65 kV, respectively. The source meter was controlled manually or through a serial port using MATLAB.

Actuation Voltage Measurements: To determine the necessary threshold of voltage to open the valve, an experimental setup was used (Figure S2, Supporting Information), containing i) a single-use valve, ii) computer-controlled voltage source (Keithly 2410 source meter, with maximum output voltage of 1.1 kV and current 100 µA), iii) a digital SLR camera (Canon EOS 550D) with video and audio recording capability equipped with macro lens kit, and iv) a personal computer, which was controlling the voltage source over RS232/USB interface. The single-use valves were prepared by bonding the electrotextile materials to a blotting paper using a thermoplastic (polyethylene) film in a hot press. A 20 µL droplet of a solution to the valve was deposited, and a source electrode wire was then placed into the droplet using a micropositioner (Thorlabs). A voltage ramp to the valve was then applied, while filming the drop, and measured the current as a function of voltage. The measurements were continued until the drop penetrated the valve. A computer program was written in MATLAB 2014 to control the voltage ramping from 0 to 1000 V at a rate of 5 V s^{-1} (total 200 s) with 10 V steps.

Measurement of Liquid Contact Angles on Teflon AF: The contact angles of different liquids using Si wafers coated with a layer of Parylene-C and Teflon-AF were determined. The contact angle of liquids was measured on the Si wafers as a function of voltage, using the same in-house built goniometry setup as described above (see Figure S2, Supporting Information).

Fabrication of Paper Devices: Paper microfluidic devices were prepared by printing wax patterns, with a Xerox ColorQube wax printer, on Whatman Chromatography paper 1. Conductors were printed on the paper using carbon ink (Ercon inc.) through stencil masks or manually. The devices were assembled using plastic films (63-µm-thick polyethylene) as a binder between the sheets. Holes were cut in the plastic films for liquid penetration. The plastic films were stacked between the papers and the electrotextiles, and hot pressed at 210 °C for 1 min to form a strong adhesion between the layers. The devices were enclosed using the same plastic film to prevent evaporation (see Figure 2).

Characterization of Valves at Different Angles vs. Gravity: Devices were fabricated by embedding aluminum textile (71 µm fiber diameter with a 10 µm Parylene C coating and a Teflon-AF coating) between two layers of paper. The paper layers had circular reservoirs (7.5 mm diameter), printed using a wax printer (a Xerox ColorQube) to confine the liquid and prevent it from sliding off the surface at different angles. Carbon ink was printed into the top reservoir as the electrode to the valve. 20 µL of an aqueous solutions containing Acid Red was placed into the reservoir and increasing voltage was applied between the electrode and the textile until the valve opened and the red dye passed through. The angle of the devices from 0° (droplet on top of paper) to 180° (droplet was hanging on the paper) was varied to analyze the behavior of the valve as a function of gravity.

Preparation and Analysis of the Iodate Assay: Circular indicator pads (7 mm diameter) were created using wax printing. 10 µL starch indicator was deposited on the pad and dried. The reagents were stored in paper in different sectors (another 7-mm-diameter circular input pad was divided into three equal areas using 2 pt line in Illustrator, a narrower line could not stop wicking) due to incompatibility between the reagents. 4 µL of 1 M p-toluenosulfonic acid, 2 µL of 0.5 M KI, and 4 µL of 30×10^{-3} M $Na_2S_2O_3$ solutions were stored in these three sectors and dried in an oven at 60 °C. An integrated device was assembled, where a preloaded indicator pad and a gate mesh were bonded using the hot pressing, and an input pad was attached using a thermal sealer, which allowed to bond surrounding areas without direct heating of the stored reagents.

The assay was tested by depositing 40 µL of sample to the input pad. A custom-built mechanical shaker shown in Figure S15 (Supporting Information) was used. After 3 min of shaking, the reagent mixture was transferred to an indicator pad. The colorimetric signal was recorded with a camera (Canon EOS 550D, EF-S 24 mm F2.8 lens), and evaluated using MATLAB, by calculating the relative change in brightness (linear sum of individual RGB channels) of the indicator area.

Supporting Information

Supporting Information is available from the Wiley Online Library or from the author.

Acknowledgements

A.A. and M.M.H. contributed equally to this work. The authors thank Chien-Chung Wang and Mohit S. Verma for their help with iodate assay. Christoph Keplinger was helpful in discussion of high voltage instrumentation. Jim MacArthur and The Electronic Instrument Design Lab (Department of Physics, Harvard University) provided an excellent environment for the development of the electronic part of the system. A.A. thanks the Swedish Research Council (VR) for a postdoctoral fellowship. M.M.H. acknowledges support from Marie Curie IOF FP7 for project nanoPAD (Grant Agreement Number 330017), the Bo Rydins stiftelse (SCA AB), and the Sweden-America Foundation. F.G. thanks the German Research Foundation (GU 1468/1-1) for research support. This work was partially funded by NSF award DMR-1420570.

Conflict of Interest

The authors declare no conflict of interest.

Keywords

electrowetting, paper microfluidics, textiles, valves

Received: May 23, 2017
Revised: July 17, 2017
Published online: August 15, 2017

[1] A. K. Yetisen, M. S. Akram, C. R. Lowe, *Lab Chip* **2013**, *13*, 2210.
[2] D. M. Cate, J. A. Adkins, J. Mettakoonpitak, C. S. Henry, *Anal. Chem.* **2015**, *87*, 19.
[3] E. W. Nery, L. T. Kubota, *Anal. Bioanal. Chem.* **2013**, *405*, 7573.
[4] J. Adkins, K. Boehle, C. Henry, *Electrophoresis* **2015**, *36*, 1811.
[5] E. J. Maxwell, A. D. Mazzeo, G. M. Whitesides, *MRS Bull.* **2013**, *38*, 309.
[6] J. Hu, S. Wang, L. Wang, F. Li, B. Pingguan-Murphy, T. J. Lu, F. Xu, *Biosens. Bioelectron.* **2014**, *54*, 585.
[7] X. Li, D. R. Ballerini, W. Shen, *Biomicrofluidics* **2012**, *6*, 011301.
[8] D. D. Liana, B. Raguse, J. Justin Gooding, E. Chow, *Sensors* **2012**, *12*, 11505.
[9] S. Ramachandran, E. Fu, B. Lutz, P. Yager, *Analyst* **2014**, *139*, 1456.
[10] A. C. Glavan, D. C. Christodouleas, B. Mosadegh, H. D. Yu, B. S. Smith, J. Lessing, M. T. Fernández-Abedul, G. M. Whitesides, *Anal. Chem.* **2014**, *86*, 11999.
[11] S. Wang, L. Ge, X. Song, J. Yu, S. Ge, J. Huang, F. Zeng, *Biosens. Bioelectron.* **2012**, *31*, 212.
[12] K. N. Han, J.-S. Choi, J. Kwon, *Sci. Rep.* **2016**, *6*, 25710.
[13] M. S. Verma, M.-N. Tsaloglou, T. Sisley, D. Christodouleas, A. Chen, J. Milette, G. M. Whitesides, *Biosens. Bioelectron.* **2018**, *99*, 77.
[14] M. Zhang, L. Ge, S. Ge, M. Yan, J. Yu, J. Huang, S. Liu, *Biosens. Bioelectron.* **2013**, *41*, 544.
[15] J. T. Connelly, J. P. Rolland, G. M. Whitesides, *Anal. Chem.* **2015**, *87*, 7595.
[16] S.-J. Lo, S.-C. Yang, D.-J. Yao, J.-H. Chen, W.-C. Tu, C.-M. Cheng, *Lab Chip* **2013**, *13*, 2686.
[17] Y. Jiang, Z. Hao, Q. He, H. Chen, *RSC Adv.* **2016**, *6*, 2888.
[18] C. K. W. Koo, F. He, S. R. Nugen, *Analyst* **2013**, *138*, 4998.
[19] P. Zwanenburg, X. Li, X. Y. Liu, in *Proc. IEEE Int. Conf. on Micro Electro Mechanical Systems*, IEEE, Taipei, Taiwan, **2013**, p. 253.
[20] M. M. Hamedi, V. E. Campbell, P. Rothemund, F. Güder, D. C. Christodouleas, J.-F. Bloch, G. M. Whitesides, *Adv. Funct. Mater.* **2016**, *26*, 2446.
[21] A. W. Martinez, S. T. Phillips, Z. Nie, C.-M. Cheng, E. Carrilho, B. J. Wiley, G. M. Whitesides, *Lab Chip* **2010**, *10*, 2499.
[22] S. Jahanshahi-Anbuhi, P. Chavan, C. Sicard, V. Leung, S. M. Z. Hossain, R. Pelton, J. D. Brennan, C. D. M. Filipe, *Lab Chip* **2012**, *12*, 5079.
[23] X. Y. Liu, C. M. Cheng, A. W. Martinez, K. A. Mirica, X. J. Li, S. T. Phillips, M. Mascareñas, G. M. Whitesides, in *IEEE 24th Int. Conf. on MEMS*, IEEE, Cancun, Mexico, **2011**, pp. 75–78.
[24] H. Chen, J. Cogswell, C. Anagnostopoulos, M. Faghri, *Lab Chip* **2012**, *12*, 2909.
[25] F. He, J. Grimes, S. D. Alcaine, S. R. Nugen, *Analyst* **2014**, *139*, 3002.
[26] T. Guo, T. Meng, W. Li, J. Qin, Z. Tong, Q. Zhang, X. Li, *Nanotechnology* **2014**, *25*, 125301.
[27] L. Cai, M. Zhong, H. Li, C. Xu, B. Yuan, *Biomicrofluidics* **2015**, *9*, 46503.
[28] R. Gerbers, W. Foellscher, H. Chen, C. Anagnostopoulos, M. Faghri, *Lab Chip* **2014**, *14*, 4042.
[29] S. Jahanshahi-Anbuhi, A. Henry, V. Leung, C. Sicard, K. Pennings, R. Pelton, J. D. Brennan, C. D. M. Filipe, *Lab Chip* **2013**, *14*, 229.
[30] B. Lutz, T. Liang, E. Fu, S. Ramachandran, P. Kauffman, P. Yager, *Lab Chip* **2013**, *13*, 2840.
[31] B. J. Toley, J. A. Wang, M. Gupta, J. R. Buser, L. K. Lafleur, B. R. Lutz, E. Fu, P. Yager, *Lab Chip* **2015**, *15*, 1432.
[32] C. C. Wang, J. W. Hennek, A. Ainla, A. A. Kumar, W. J. Lan, J. Im, B. S. Smith, M. Zhao, G. M. Whitesides, *Anal. Chem.* **2016**, *88*, 6326.
[33] J. Ding, B. Li, L. Chen, W. Qin, *Angew. Chem. Int. Ed.* **2016**, *55*, 13033.
[34] B. Lu, S. Zheng, B. Q. Quach, Y.-C. Tai, *Lab Chip* **2010**, *10*, 1826.
[35] J. B. Fortin, T.-M. Lu, *J. Vac. Sci. Technol., A* **2000**, *18*, 2459.
[36] DuPont, Amorphous Fluoroplastic Resin Teflon® AF- Datasheet.
[37] A. A. Mariod, H. F. Adam, *Acta Sci. Pol., Technol. Aliment.* **2013**, *12*, 135.
[38] D. Chatterjee, B. Hetayothin, A. R. Wheeler, D. J. King, R. L. Garrell, *Lab Chip* **2006**, *6*, 199.
[39] S. K. Cho, H. Moon, C. J. Kim, *J. Microelectromech. Syst.* **2003**, *12*, 70.
[40] S. Urazhdin, N. O. Birge, W. P. Pratt, J. Bass, *Phys. Rev. Lett.* **2003**, *91*, 146803.
[41] H. Moon, S. K. Cho, R. L. Garrell, C. J. Kim, *J. Appl. Phys.* **2002**, *92*, 4080.
[42] F. Mugele, J.-C. Baret, *J. Phys.: Condens. Matter* **2005**, *17*, R705.
[43] P. Paik, V. K. Pamula, M. G. Pollack, R. B. Fair, *Lab Chip* **2003**, *3*, 28.
[44] M. G. Pollack, A. D. Shenderov, R. B. Fair, *Lab Chip* **2002**, *2*, 96.
[45] A. R. Wheeler, H. Moon, C. a. Bird, R. R. O. Loo, C. J. Kim, J. a. Loo, R. L. Garrell, *Anal. Chem.* **2005**, *77*, 534.
[46] A. R. Wheeler, *Science* **2008**, *322*, 539.
[47] K. H. Kang, *Langmuir* **2002**, *18*, 10318.
[48] V. Peykov, A. Quinn, J. Ralston, *Colloid Polym. Sci.* **2000**, *278*, 789.
[49] M. Vallet, M. Vallade, B. Berge, *Eur. Phys. J. B* **1999**, *11*, 583.
[50] E. W. Washburn, *Proc. Natl. Acad. Sci. USA* **1921**, *7*, 115.
[51] M. M. Hamedi, A. Ainla, F. Güder, D. C. Christodouleas, M. T. Fernández-Abedul, G. M. Whitesides, *Adv. Mater.* **2016**, *28*, 5054.
[52] E. Carrilho, A. W. Martinez, G. M. Whitesides, *Anal. Chem.* **2009**, *81*, 7091.

[53] F. Güder, A. Ainla, J. Redston, B. Mosadegh, A. Glavan, T. J. Martin, G. M. Whitesides, *Angew. Chem. Int. Ed.* **2016**, *128*, 5821.
[54] A. Nemiroski, D. C. Christodouleas, J. W. Hennek, A. A. Kumar, E. J. Maxwell, M. T. Fernández-Abedul, G. M. Whitesides, *Proc. Natl. Acad. Sci. USA* **2014**, *111*, 11984.
[55] N. M. Myers, E. N. Kernisan, M. Lieberman, *Anal. Chem.* **2015**, *87*, 3764.
[56] M. Focke, D. Kosse, C. Müller, H. Reinecke, R. Zengerle, F. von Stetten, *Lab Chip* **2010**, *10*, 1365.
[57] S. Lutz, P. Weber, M. Focke, B. Faltin, J. Hoffmann, C. Müller, D. Mark, G. Roth, P. Munday, N. Armes, O. Piepenburg, R. Zengerle, F. von Stetten, *Lab Chip* **2010**, *10*, 887.
[58] M. M. Thuo, R. V. Martinez, W. J. Lan, X. Liu, J. Barber, M. B. J. Atkinson, D. Bandarage, J. F. Bloch, G. M. Whitesides, *Chem. Mater.* **2014**, *26*, 4230.
[59] A. C. Glavan, R. V Martinez, E. J. Maxwell, A. B. Subramaniam, R. M. D. Nunes, S. Soh, G. M. Whitesides, *Lab Chip* **2013**, *13*, 2922.
[60] C. Renault, X. Li, S. E. Fosdick, R. M. Crooks, *Anal. Chem.*, **2013**, *85*, 7976.
[61] M. A. Unger, H. Chou, T. Thorsen, A. Scherer, S. R. Quake, *Science* **2000**, *288*, 113.
[62] B. Mosadegh, A. D. Mazzeo, R. F. Shepherd, S. A Morin, U. Gupta, I. Z. Sani, D. Lai, S. Takayama, G. M. Whitesides, *Lab Chip* **2014**, *14*, 189.

